

高分子材料への電荷注入過程とその評価 I

高分子材料のキャリアトラップ

小 嶋 憲 三

Carrier Injection Processes into Polymers and Their Evaluations I

Carrier Traps in Polymers

Kenzo KOJIMA

1. Thermally stimulated currents (TSC) from polyethylene terephthalate (PET) electrets formed by high electric fields were investigated. Electrons injected from the Al cathode greatly contribute to the TSC above -40°C , the TSC below -40°C for Al electrodes and at all temperatures for Au electrodes are mainly induced by the depolarization of dipoles.

2. Carrier traps in PET, PEN, PE, PP and PVDF were investigated by TSC and TL analysis in the temperature range from -196 to 100°C . The electron beam with energy of 2~5 keV irradiated specimens to form electrets at -196°C . It was proved that the electron beam technique was useful for the investigation of carrier traps in vinyl polymers with no π electron groups.

3. Electronic carrier traps in PET and PEN were investigated by photoexcitation techniques. A broad peak was observed in temperature range from -160 to 50°C in PET photoelectrets illuminated at 300 nm at -180°C . Their apparent trap depth was found to distribute from 0.2 to 0.5 eV. On the other hand, two broad peaks were observed in the TSC and TL from PEN photoelectrets illuminated at 360 nm. Their apparent trap depths ranged from 0.1 to 0.5 eV.

Introduction

Analysis of thermally stimulated currents (TSC) has been frequently employed to investigate the molecular motions and carrier trapping phenomena in polymeric materials.¹⁾

It is quiet needed to study these phenomena for understanding the fundamental properties of electrical insulating materials.

In general, TSC's from thermoelectrets are considered to be induced by the thermal release of dipoles, ions and trapped electrons. It is not so easy to distinguish which of these origins contribute to the TSC peaks, because the extent of each contribution is expected to depend on the forming condition of electrets.

Several forming techniques of electrets were proposed to discuss separately these origins of the TSC. For example, thermoelectrets formed by applying a low field at high temperature are often studied to understand the depolarization properties of

dipoles.²⁾

On the other hand, photoelectrets excited with ultraviolet light,³⁾ radioelectrets with γ -rays⁴⁾ or X-rays⁵⁾ and electrets formed with electron beam⁶⁾ are frequently investigated to identify the trapping parameters of electronic carriers. Injected or excited carriers are captured by traps located at the surface or in the bulk of polymers. These trapped carriers are thermally released and drift through the bulk of a specimen under an electric field, resulting in currents called TSC.

On the other hand, thermally detrapped carriers may recombine with ionized parent molecules, causing light emission, called TL.

In this paper, electron trapping properties of PET, PEN and other polymers were discussed by analyzing the TSC and TL in the electrets formed by (1) electrical high field, (2) electron beam irradiation and (3) photoexcitation.

Specimens

Specimens investigated are commercial films,

Table 1. Specimens Investigated

Specimen	Code	Formula
Polyethylene Terephthalate	PET	$\left[-O-\text{C}(=\text{O})-\text{C}_6\text{H}_4-\text{C}(=\text{O})-\text{O}-(\text{CH}_2)_2 \right]_n$
Polybutylene terephthalate	PBT	$\left[-O-\text{C}(=\text{O})-\text{C}_6\text{H}_4-\text{C}(=\text{O})-\text{O}-(\text{CH}_2)_4 \right]_n$
Polyethylene naphthalate	PEN	$\left[-O-\text{C}(=\text{O})-\text{C}_{10}\text{H}_6-\text{C}(=\text{O})-\text{O}-(\text{CH}_2)_2 \right]_n$
Polyethylene	PE	$\left[\begin{array}{c} \text{H} & \text{H} \\ & \\ \text{C} & - & \text{C} \\ & \\ \text{H} & \text{H} \end{array} \right]_n$
Polypropylene	PP	$\left[\begin{array}{c} \text{H} & \text{H} \\ & \\ \text{C} & - & \text{C} \\ & \\ \text{H} & \text{CH}_3 \end{array} \right]_n$
Polyvinylidene fluoride	PVDF	$\left[\begin{array}{c} \text{H} & \text{F} \\ & \\ \text{C} & - & \text{C} \\ & \\ \text{H} & \text{F} \end{array} \right]_n$

Table 2. Physical Properties of PET

glass transition temp. (T_g)	85°C
melting point (T_m)	250°C
specific gravity	1.38
crystallinity (X_c)	41%
water absorption	0.3%
dielectric constant 20°C, 100Hz	3.3
dielectric loss factor 20°C, 100Hz	0.01

Table 3. Physical properties of PEN

glass transition temp. (T_g)	110~120°C
melting point (T_m)	270°C
crystallinity (X_c)	45%
dielectric constant 20°C, 100Hz	3.2
dielectric loss factor "	0.01

which are summarized in table 1. Aromatic polyesters, such as polyethylene terephthalate (PET) and polyethylene naphthalate (PEN) were mainly investigated. Their physical properties are also summarized in table 2 and 3.

1 TSC in Field-Induced Electrets

1-1 Experimental

The specimens studied are 12 μm thick commercial films of PET having a sandwich structure of Au-PET-Au and Au-PET-Al with evaporated metal electrodes of 3 cm diameter. Figure 1 shows the electrode arrangements and the block diagram for measuring TSC. All experiments were carried out in vacuum of less than 1×10^{-4} Pa.

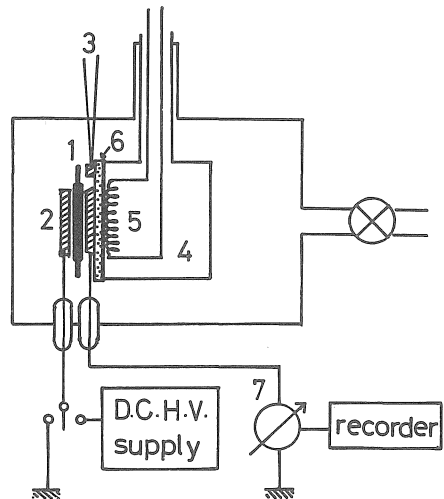


Fig. 1. Block diagram of the apparatus for measuring TSC. 1: specimen, 2: electrode (Cu), 3: thermocouple (CA), 4: liquid N_2 , 5: heater, 6: insulator (boron nitride), 7: vibrating reed electrometer.

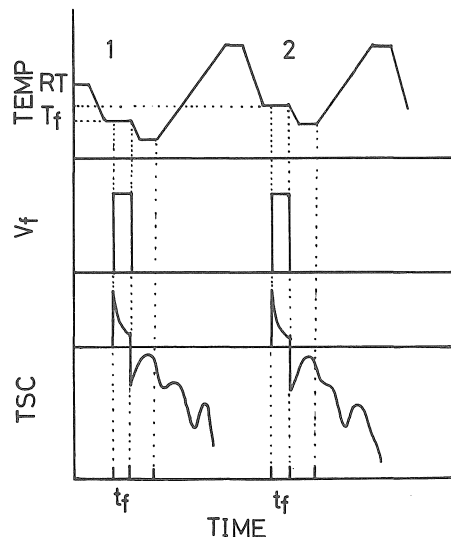


Fig. 2. Experimental procedure for measurements of TSC.

The thermal sampling technique¹⁾ was employed at various temperatures from -190 to 120°C . The forming procedures of electrets are shown in Fig. 2 schematically. After a forming voltage (V_f) is applied to the specimen for a period (t_f) at a temperature (T_f), the specimen is short-circuited and abruptly cooled down to a certain temperature. TSC's are measured by heating the specimen at a constant rate (β) with the specimen short-circuited. Experiments were usually carried out under the condition of $V_f = 1.2$ kV, $t_f = 10$ sec and $\beta = 5^\circ\text{C}/\text{min}$ which was referred to as the standard condition.

1-2 Results and Discussion

TSC spectra of thermoelectrets of PET have been reported to have two peaks below $+120^{\circ}\text{C}$ ¹. One peak appears a little above T_g (glass transition temperature) and another one around -100°C . These correspond to the α and β dispersions respectively observed in dielectric measurements and interpreted by the depolarization of dipoles. Recently, the TSC in much higher temperature range than T_g was investigated which was explained from ionic polarization.⁷⁾

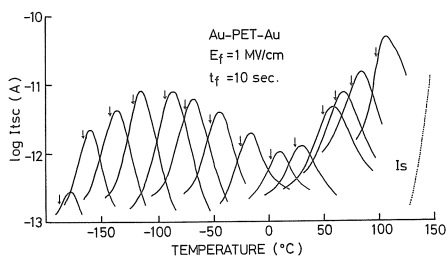


Fig. 3. TSC spectra obtained by thermal sampling technique from Au-PET-Au electret. I_s : short-circuit current.

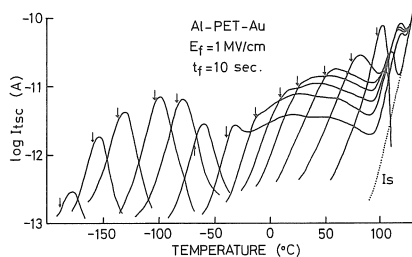


Fig. 4. TSC spectra obtained from Au-PET-Al electret. I_s : short-circuit current.

In this paper we studied the TSC below T_g chiefly. The TSC spectra of Au-PET-Au electret formed at various temperatures under the standard condition are shown in Fig. 3 where the arrow shows the forming temperature T_f of each curve. Each TSC curve shows only one peak at the temperature a little above the T_f in all experimental temperature range. Moreover, the peak intensity shows a maximum around -100°C and increases above 0°C . On the other hand, the TSC spectra of Au-PET-Al electrets were very different from those of Au-PET-Au electrets. Figure 4 shows the TSC obtained from Au-PET-Al electret formed by applying a negative voltage to the Al electrode. For forming temperatures below -40°C the TSC spectra are very similar to those obtained from Au-PET-Au electret.

However, each TSC above -40°C showed new broad peaks in much higher temperature range than the T_f . The apparent activation energies of Au-PET-Au electret were estimated to be in the range from 0.2 to 2.0 eV from each curve shown in Fig. 3 using the initial rise method. On the other hand, those of Au-

PET-Al electret were evaluated by applying the partial heating technique to the electret formed at -40°C . This is because the TSC shows a broad peak well above T_f in addition to the peak at slightly higher temperature than the T_f . These results are shown in Fig. 5. Significant difference was not observed between both activation energies.

The polarity effect of forming voltage on the TSC of Au-PET-Al electret formed at -40°C was investigated. The result is shown in Fig. 6. In the case of a negative forming voltage to Al electrode, three peaks (P_1 , P_2 and P_3) appeared in the TSC spectra, while in the case of a positive forming voltage, only a peak (P'_1) was observed a little above T_f and no broad peaks corresponding to P_2 and P_3 were recognized. The P_1 and P'_1 peaks appear at the same temperature. Their intensities are independent of the polarity of the forming voltage and in proportion to V_f . The polarity effect was clearly observed in the electret formed under a high field more than 1 MV/cm. Under a low forming field P_1 is dominant in the TSC spectra, while both peaks P_2 and P_3 became larger than P_1 as the field increases.

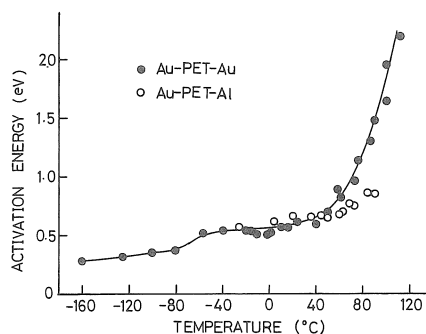


Fig. 5. Apparent activation energies of TSC. ● : estimated from each TSC in Fig.3, ○ : estimated from the TSC in Au-PET-Al electret formed at -40°C by partial heating technique.

Hino *et al.*^{1,8)} obtained a similar TSC in the PET electret formed under the low field by one order of magnitude than that employed in this experiment, and they explained it by thermal depolarization of dipoles.

The molecular motion of PET was investigated in detail by Illers *et al.*⁹⁾ by using mechanical method. They observed the γ dispersion at -165°C by methylene group and the β dispersion at -105 and -70°C by carbonyl group.

The present results obtained from Au-PET-Au electret may be also concluded to be mainly due to the thermal depolarization of dipoles, and it is also supposed that the TSC from Au-PET-Al electret at temperatures below -40°C is caused by dipoles because it shows no electrode effects. This is also supported by the following fact. According to Hino *et al.*⁸⁾ the frequency factor K can be calculated from

eq. (1) which was presented for the dipolar single relaxation case

$$\log K = 0.434[(H/kT_m) - \ln(2kT_m^2/\beta H)]. \quad (1)$$

where H , T_m , k and β are the activation energy, maximum temperature, Boltzmann's constant and heating rate, respectively.

Substituting experimental values of H , T_m and β , $\log K$ was calculated at 10.1~10.6 which well agrees with the results obtained by Hino *et al.*⁸⁾

On the other hand, a remarkable electrode dependence of the TSC from Au-PET-Al electret formed above -40°C is difficult to be explained by dipoles.

Lilly *et al.*¹⁰⁾ observed the complicated TSC in Mylar electret formed with high field pulses at room temperature, which was strongly affected by the electrode metals. It was explained by the double injection of electrons and holes from electrodes into the bulk and/or surface of specimen. The TSC's due to the injected charge from electrodes were also observed in PE and oxidized PE electrets formed with DC high field.¹¹⁾¹²⁾

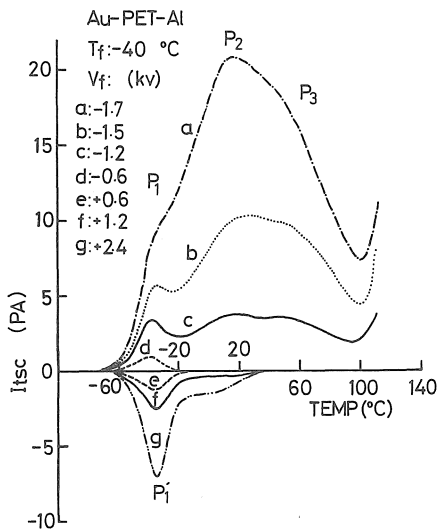


Fig. 6. Polarity effects of forming field on the TSC spectra of Au-PET-Al electret.

The forming field of 1 MV/cm used in this experiments is supposed to be sufficiently large to induce the electron injection from cathode into PET. The broad peaks observed above -40°C in the TSC from Au-PET-Al electret is considered to be induced by the release of trapped electrons which have been injected from Al electrode under a negative high field, because such a peak can be scarcely observed in the TSC from Au-PET-Au electret. The peaks P_2 and P_3 strongly depend upon the polarity of the forming voltage and they are remarkably enhanced when the negative forming voltage was applied to Al electrode having a low work function compared with that of Au. These

are shown in Fig. 7 which gives charge Q estimated from the TSC peak area against forming field, where Q_1 shows the dipolar peak P_1 and Q_2 contains both electronic peaks P_2 and P_3 together. The charge Q_1 has a linear relations, but Q_2 has a more complicated ones with forming field. The apparent injected charge Q_2 can be scarcely observed until the forming field increased to 0.8 MV/cm, and then shows an abrupt increase with the field. The magnitude of the field may be reasonable as the on set field of electron injection from Al electrode.¹²⁾

As shown in Fig. 5, the activation energies of depolarization of dipoles almost coincided with the trap depths of the electronic traps. This may be possible to consider that the detrapping process of trapped electrons are strongly affected by the molecular motion. Whereas complementary experiments with the collecting field showed that the broad peak shifted towards low temperature as the field increased. This can not be explained from the model which takes only the molecular motion into account on the carrier detrapping process.

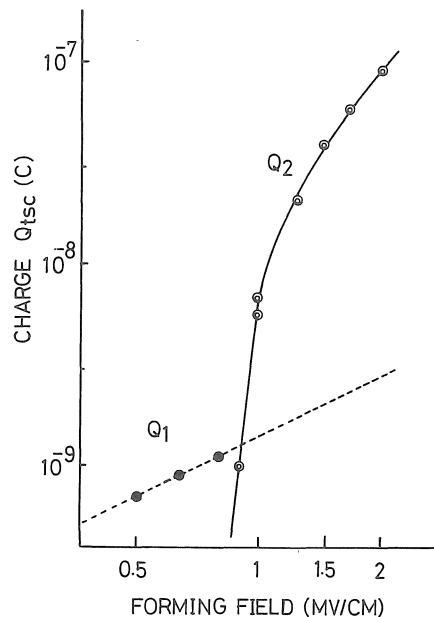


Fig. 7. Forming field dependence of apparent collected charge from Au-PET-Al electret. Q_1 : evaluated from P_1 , Q_2 : evaluated totally from P_2 and P_3 in Fig. 6.

The P_2 (P_3) peak shifted about 40°C towards low temperature by the collecting fields (0.17~0.83 MV/cm) as shown in Fig. 8. The temperature shift of TSC peaks by an external field has been observed in many polymers,¹³⁾ and is one of the characteristics of TSC due to carriers. Zielinski *et al.*¹⁴⁾ analyzed it according to the Pool-Frenkel effect in detrapping processes. The peak temperature (T_m) is given eq. (2) after

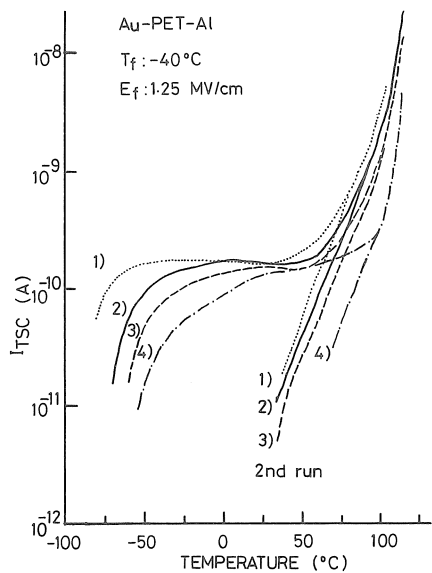


Fig. 8. Peak shifts due to collecting field (E_c)
 1) 0.83MV/cm 2) 0.63MV/cm
 3) 0.42MV/cm 4) 0.17MV/cm

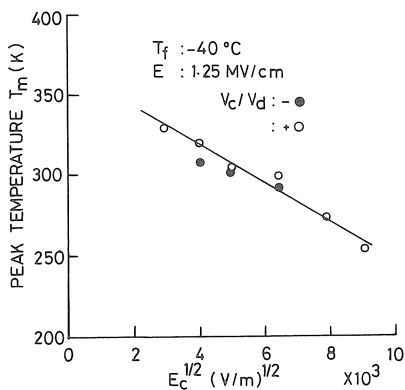


Fig. 9. Shift of TSC peaks due to applied field E_c

Zeilinski.

$$T_m = \frac{E}{k \ln(\nu k T_m^2 / \beta E)} \quad (2)$$

where E is the trap depth, β is the rising rate of temperature, ν is the attempt-to-escape frequency and k is Boltzmann's constant. If E_0 is the trap depth with no field, E is expressed as $E_0 - \beta_{pF} F^{1/2}$. Therefore eq. (2) becomes eq. (3).

$$T_m = E_0 / kC - \beta_{pF} F^{1/2} / kC \quad (3)$$

where, $C = \ln[\nu k T_m^2 / \beta (E_0 - \beta_{pF} F^{1/2})]$
 T_m is plotted as a function of $F^{1/2}$, according to the eq. (3), in Fig. 9. The slope of the straight line, β_{pF} / E_0 was estimated at $3.5 \times 10^{-5} (\text{m}^{1/2} \text{V}^{-1/2})$. Substituting 0.75 eV for E_0 , β_{pF} was evaluated at $2.6 \times 10^{-5} (\text{eV m}^{1/2} \text{V}^{-1/2})$. On the other hand, the theoretical value of β_{pF} ($\epsilon_r = 3$)

is $4.4 \times 10^{-5} (\text{eV m}^{1/2} \text{V}^{-1/2})$ which differs from the experimental value of 2.6×10^{-5} , by factor of 1.7. Although, the peak shifts in PET was not explained quantitatively by the Pool-Frenkel model, the P_2 (P_3) peaks were clarified as originating from released carriers. However, the exact process of detrapping is not clear yet and further investigation on the trap of PET will be required.

2 TSC and TL in Electron Beam-Irradiated Electrets

2-1 Experimental

Two kinds of measurements were carried out in this section. One is the measurement of luminescence spectrum during irradiation of electron beam. The other is the TSC and TL measurements after irradiation of electron beam.

1) Luminescence Spectrum

Luminescence spectra of PET, PBT and PEN were observed by a photomultiplier (HTV, R432) through a monochromator (Shimazu-Boush & Lomb) during the irradiation of electron beam at liquid nitrogen and room temperatures (Fig. 10).

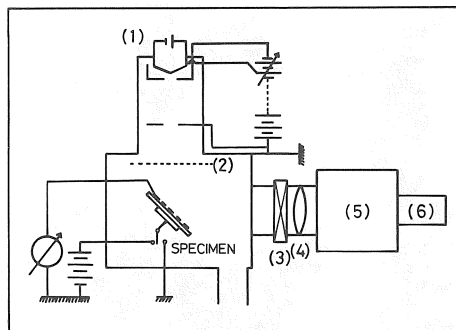


Fig. 10. Schematic diagram of the experimental apparatus for measurement of luminescence spectra, TSC and TL excited by electron beam. 1) electron gun 2) Al foil 3) shutter 4) lens 5) monochromator and 6) photomultiplier

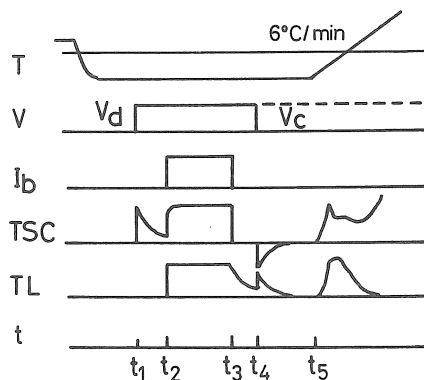


Fig. 11. Experimental procedure for measurements of TSC and TL.

2) TSC and TL

Gold electrodes were prepared on the both sides of specimens by vacuum evaporation. Electron beam (accelerating voltage V_{acc} , beam current I_b) was pre-irradiated through the semitransparent front gold electrode for 10 minutes at liquid nitrogen temperature.

TSC and TL were measured simultaneously by heating the specimen at constant rate of $6^\circ\text{C}/\text{min}$ (Fig. 11).

2-2 Results and Discussion

1) Luminescence

Photograph 1 shows a luminescence in PEN during irradiation of electron beam ($V_{acc} = 5\text{ kV}$, $I_b = 1 \times 10^{-7}\text{ A}$, beam radius 10 mm).

In general, very weak luminescence is observed in insulating polymers. Aromatic polymers, having π electron group, however, emit relatively intense luminescence enough to be visible in human eyes.

The luminescence intensities of PET and PEN were in proportion to the beam current irrespective of temperature and accelerating voltage. The luminescence

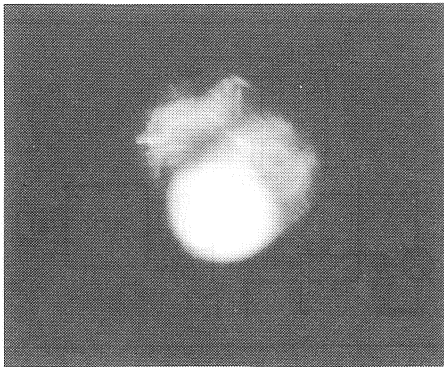


Photo. 1. photograph of luminescence in Au-PEN-Au excited by electron beam (5 KeV, $1 \cdot 10^{-7}\text{ A}$).

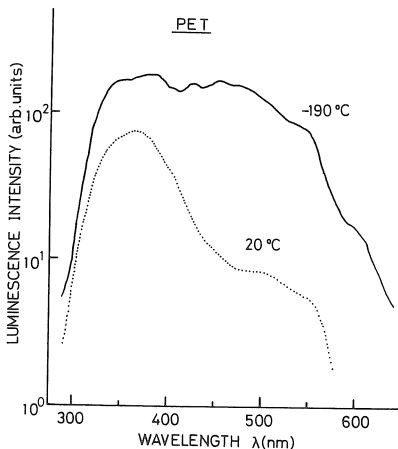


Fig. 12. Luminescence spectra in PET excited by electron beam (4 KeV).

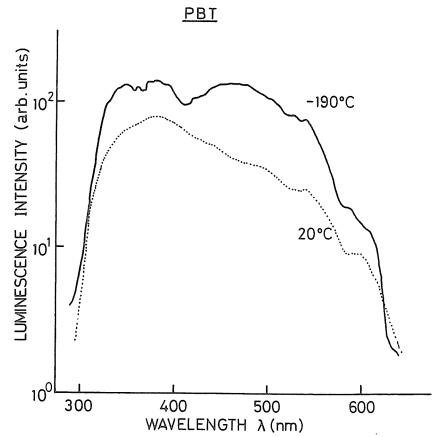


Fig. 13. Luminescence spectra in PBT irradiated by electron beam (5 KeV).

scence spectra of PET, PBT and PEN were shown in Figs. 12~14, respectively. Two emission bands centered at 375 and 450 nm were observed in PET at liquid nitrogen temperature. The emission intensity in visible region decreased remarkably with increasing temperature comparing to that of ultraviolet region. The similar spectrum and temperature dependence were observed in PBT to that of PET. These results suggest that the luminescence originates from the π electron groups in the molecular structure of polymers, because these two polymers have the same π electron group ($-\text{C}(=\text{O})-\text{C}_6\text{H}_4-\text{C}(=\text{O})-$).

The strong emission at 410 and a weak one at 580 nm were observed in PEN at liquid nitrogen temperature. The emission at 410 nm shifted to 425 nm at

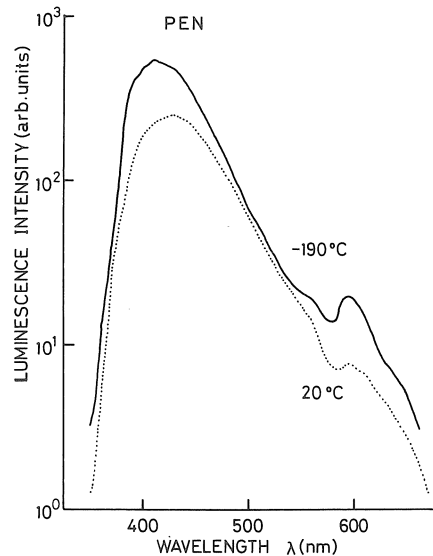


Fig. 14. Luminescence spectra in PEN excited by electron beam (4 KeV).

room temperature (20°C).

Schug *et al.*¹⁵⁾ have reported on the cathode luminescence in aromatic polymers such as PET, PEN and PPX (poly-p-xylylene) at room temperature. The emission spectra of PET and PEN at room temperature are in good agreement with their results.

The photoluminescence of these aromatic polyesters have been well understood.¹⁶⁾ The monomer fluorescence ($M^* \rightarrow M + h\nu_M$) at 335 nm and excimer fluorescence ($D^* \rightarrow 2M + h\nu_e$) at 375 nm have been observed in PET excited by UV light (300 nm).¹⁷⁾

On the other hand, the excimer fluorescence and phosphorescence have been observed at 410 and 580 nm in PEN excited at 360 nm. The luminescence spectra shown in Figs. 12~14 agreed with those photoluminescence spectra. This suggests that the emission processes of cathode ray luminescence are also resulted from energy transition of excited electron in the lowest excited state to their ground state.

2) TSC and TL in PET

Two broad peaks (P_1, P_2 and L_1, L_2) were observed on the TSC and TL curves, respectively, as shown in Fig. 15. TL is considered to result from recombination of ionized molecules and electrons released from

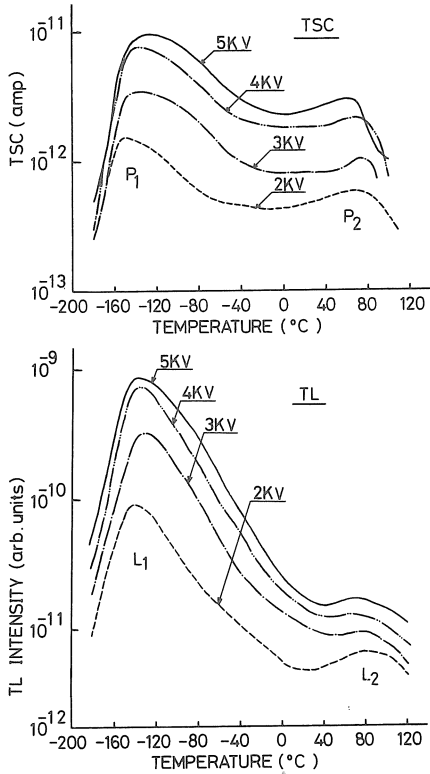


Fig. 15. TSC and TL spectra in PET excited by the electron beam with various accelerating voltage : $I_b = 1 \times 10^{-8}$ A, 10 min, with the front electrode open-circuited.

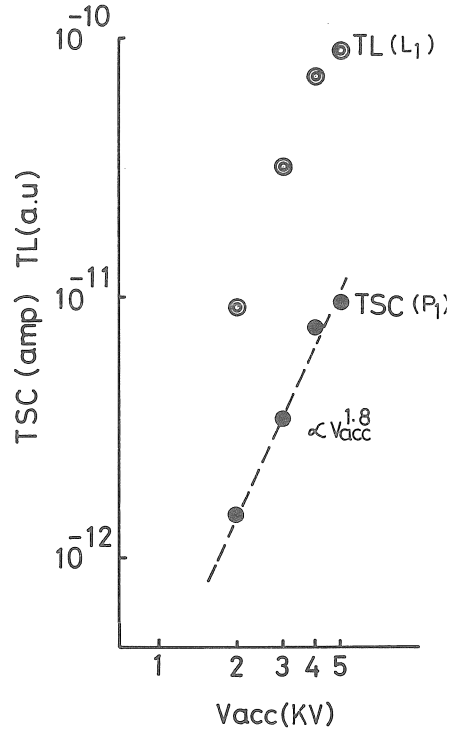


Fig. 16. TSC and TL maxima as a function of accelerating voltage V_{acc} .

traps by thermal energy. The TSC peaks, corresponding to the TL peaks, are ascribed to release of trapped electrons from shallow and deep traps, the trap depths were estimated from initial rise method¹⁸⁾ at 0.2 and 0.6 eV, respectively. Release of trapped electron were enhanced by molecular motions, the P_1 and P_2 peaks are supposed to be concerned with γ, β and α relaxation, respectively.

The peak intensities of TSC (P_1) and TL (L_1) were plotted in Fig. 16 as a function of the accelerating voltage (V_{acc}) of incident electron beam. P_1 and L_1 were proportional to V_{acc}^n ($n=1.8 \sim 2$). This relationship were considered to be connected with the penetration depth of incident electron beam by following considerations. The penetration depth (l) of electrons into PET film has been reported as follows,¹⁹⁾

$$l = 4 \times 10^{-8} E^{1.775} \quad (4)$$

where E is the mean energy of incident electrons. The energy of electrons in our experiments was less than 5 keV, therefore, the penetration depth (l) should be less than $1 \mu m$ by eq. (4).

Assuming the uniform charge distribution (ρ_0) of $1 \mu m$ in thickness, the induced charge Q on the irradiated front electrode were calculated as follows.

$$Q = S \int_0^a \frac{d-x}{d} \rho(x) dx = \left(1 - \frac{l}{2a}\right) \rho_0 S \quad (5)$$

where d is thickness of specimen, S diameter of incident electron beam and $\rho(x)$ charge density at x (m) from the front electrode. considering $l = 0.7 \mu\text{m}$ estimated from eq. (4) for $E = 5 \text{ keV}$, the condition $l \gg \frac{1}{2a}$ was satisfied in eq. (5), then, the relationship $Q \propto E^{1.775}$ is obtained.

In the following, the effect of collecting field on the recombination process was discussed. TL intensities were quenched by application of external fields, irrespectively of its polarity as shown in Fig. 17. The polarity effect, however, was observed. The degree of TL quenching by the external field was more remarkable in the positive bias which drifts the released electron into bulk from the irradiated electrode.

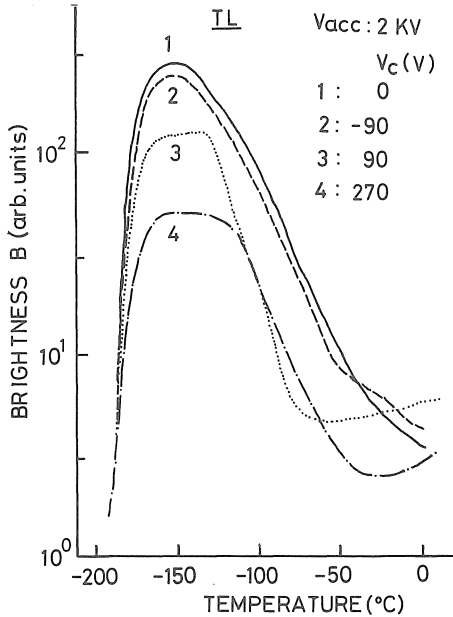


Fig. 17. TL spectra obtained with collecting bias V_c .

In the case of photoexcited TL, these field quenching phenomena have already discussed²⁰⁾ according to the Onsager's theory on the ionization probability. The distance between a parent ion and an electron in PET was estimated at 80 \AA by Takai *et al.*²⁰⁾

In the present case, the polarity effect which can not be explained by Onsager's model, is one distinct point from the photoexcited TL. Then, the qualitative explanation for the field quenching phenomena with

polarity effect was considered in the following. The surface layer of PET film is ionized by collision of incident electrons. The incident (primary) and generated (secondary) electrons were trapped in adjacent of parent ions. In the heating step, these trapped electrons were released and recombine with parent ions under their coulombic field in absence of external field, and emitting TL. On the other hand, the bulk recombination is reduced because some of the released electrons are drifted from ionized layer into bulk by application of positive bias. When a negative bias was applied, released electrons are drifted within the ionized layer towards irradiated front electrode, then, the bulk recombination is scarcely quenched.

It is reasonable to suppose the polarity effect is remarkable in the case of electron beam excited TL, because relatively high density of electrons and ions are generated, and consequently the bulk recombination dominates the geminate recombination mainly observed in the photoelectret.

3) TSC and TL in Other Polymers

TSC and TL are observed in some vinyl polymers which have no π electron, such as polyethylene (PE), polypropylene (PP) and polyvinylidene fluoride (PVDF), from the electron beam technique (Fig. 18). These results are summarized in table 4.

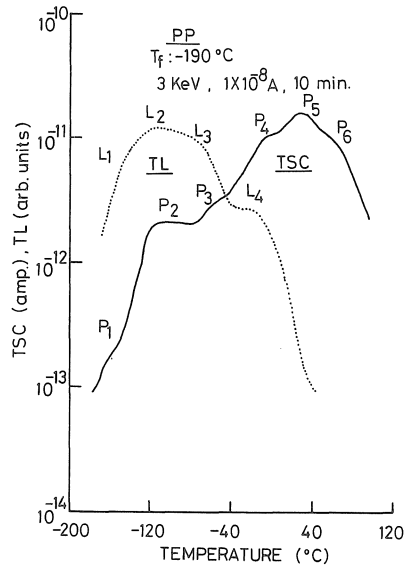


Fig. 18. TSC and TL spectra of PP.

Table 4. TSC and TL peaks

Sample	TSC Peaks (°C)						TL Peaks (°C)			
	P_1	P_2	P_3	P_4	P_5	P_6	L_1	L_2	L_3	L_4
HDPE	-140	-100	-40	0	20	65	-130	-100	-40	40
PP	-160	-120	-50	0	30	65	-145	-115	-75	-15
PVDF	-140	-75	-22	13			-140	-67	0	

These results suggest that several kinds of carrier traps exist in the specimen. The detailed discussion about the origin of carrier traps, however, was abbreviated in the present paper. It is noticed that the electron beam excitation is one of the useful method to analyze the carrier traps in vinyl polymers with no π electron group.

3 TSC and TL in Photoelectrets

3-1 Experimental

PET and PEN films $12\mu\text{m}$ in thickness were used for the investigation. Electrodes, one of which was semitransparent, were prepared on both sides of a specimen by the evaporation of Au or Cu for PET and Au or Al for PEN. The specimen was mounted on a temperature-controlable electrode system in a vessel evacuated to a pressure of less than 10^{-4} Pa.

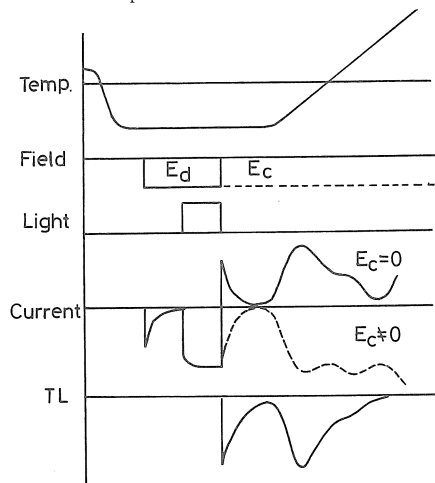


Fig. 19. Experimental procedure.

Since PET and PEN are excited into the lowest excited singlet state by light at 300 and 360 nm, respectively, their optical transition were shown in table 5. The specimen was illuminated by these monochromatic light under an electric field (E_d) at liquid nitrogen temperature, then both light and field were removed at the same time. The TSC and TL were measured by heating at a rate of $5^\circ\text{C}/\text{min}$ with or without a collecting bias (E_c), after transient currents and after-glow emission decayed to a negligible level. These experimental procedures are illustrated in Fig. 19. The TL was measured with a photomultiplier tube (R 292, HTV) connected to a vibrating-reed electrometer (TR 84M, Takeda Riken). Also, to investigate the molecular motions of PEN, the dielectric propert-

Table 5. Optical transition of PET and PEN

Materials	${}^1E_{1u} - {}^1A_{1g}$	${}^1B_{1u} - {}^1A_{1g}$	${}^1B_{1u} - {}^1A_{1g}$
PEN	200	260p	300p
PEN	244p	290p	380p

ies were measured with a capacitance bridge (Model 1238, G.R.) at the same heating rate as for the TSC measurement and at frequencies from 100 Hz to 10 kHz.

3-2 Results and Discussion

1) PET Photoelectrets

Thermally stimulated currents have been extensively investigated to understand trapping phenomena in polymers. In general, polymer electrets are formed by an application of a high field at high temperature, a corona discharge or a high energy radiation (γ -ray, X-ray, electron beam etc.). There is no report on the thermally stimulated current (TSC) in the polymer electret formed by the photo-excitation so far as the authors know.

Polyethylene terephthalate (PET) shows a remarkable photoconduction in the ultraviolet wavelength range. The photoconduction has been found to be induced by electrons generated through an excitonic excitation in the wavelength range from 200 nm to 320 nm and also by electrons photo-injected from metal electrodes,²¹⁾ especially from Cu and Al electrodes in the range longer than 320 nm (Fig. 20). Therefore, the photo-excitation of PET in the ultraviolet wavelength range under a bias field at low temperature will lead to the formation of a photoelectret through trapping the photo-induced carriers. Then, the analysis of TSC in the photoelectret gives a significant advance to understanding the electronic trap centers in PET.

The PET photoelectret was formed at about -180°C under a field of 4×10^5 V/cm by illuminating with a

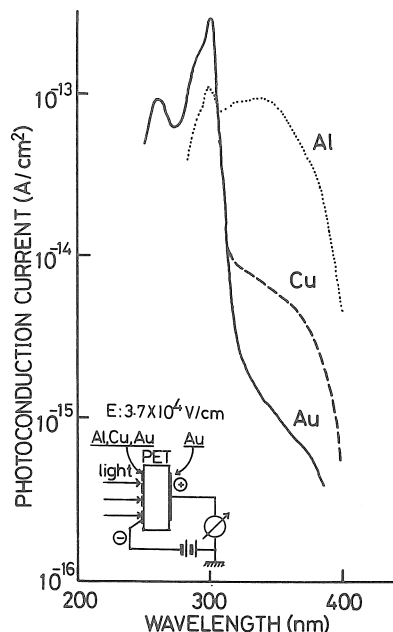


Fig. 20. Electrode effects on photocurrents in PET (3.7×10^4 V/cm in air) after Takai²¹⁾.

monochromatic light. Then, the photoelectret was heated at a rate of 6°C/min. with no bias voltage. All measurements were carried out in 10^{-3} Torr.

Typical TSC curves are shown in Fig. 21. Curves (1) and (2) were obtained on the photoelectrets with Au and Cu electrodes by illuminating the negative electrode for 30 minutes with a light of 300 nm corresponding to ${}^1B_{2u} \leftarrow {}^1A_{1g}$ excitation in PET (Table 5). Curves (3) and (4) were obtained on the electrets formed only by the electric field of 4×10^5 V/cm with no illumination. In all cases, the electric field was applied for an hour.

In Fig. 21 TSC [curve (2)] obtained in the photoelectret with a Cu electrode formed by illuminating the negative electrode with a light of 350 nm corresponding to the photoelectron injection from a metal electrode is shown together with the curves (1) and (3) in Fig. 21.

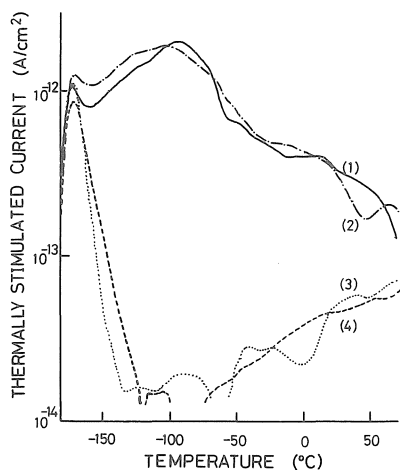


Fig. 21. TSC in photoelectrets compared with the electrets formed without the light. Curves (1) and (2): TSC in the photo-electrets with Au and Cu electrodes, respectively, which were formed by the photo-excitation (300nm) at 4×10^5 V/cm. Curves (3) and (4): TSC in the electret formed only by the electric field of 4×10^5 V/cm for the cases of Cu and Au electrodes, respectively.

In both figures, the sharp peak can be observed around -170°C . This peak is concluded to be due to the dipole depolarization, because it is independent of the electrode materials [Fig. 21 (3), and (4)], and the photo-injection from a Cu electrode gives no increase of this peak height [Fig. 22 (2)], and also the polarity effect is not observed.

The difference between curves (1), (2) and (3), (4) in Fig. 1 clearly shows the thermal release of the trapped photoelectrons. It is because the photoelectrets were formed by the bulk excitation (300 nm) that curves (1) and (2) in Fig. 21 scarcely show any differences. The photo-injection current from a Cu electrode at 350 nm is smaller by about one order than

the photocurrent under the bulk excitation at 300 nm, which indicates that photocarriers are induced more effectively by the bulk excitation than the photo-injection. This is why the photoelectret formed with a light of 350 nm shows a smaller TSC than that formed with a light of 300 nm. (See Fig. 22).

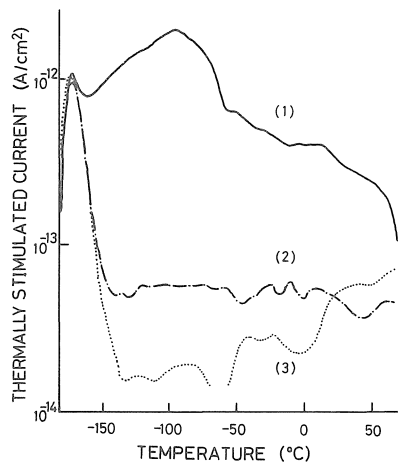


Fig. 22. TSC [curve (2)] in the photoelectret formed by the photo-injection from a Cu electrode, together with the TSC curves (1) and (3) in Fig. 21.

The apparent trap depth was found to be distributed from 0.2 eV ($\sim -150^\circ\text{C}$) to 0.5 eV ($\sim 0^\circ\text{C}$) by the partial heating technique. More detailed features of the traps are now under investigation.

2) PEN Photoelectrets

The TSC from PEN photoelectrets showed two peaks, P_1 and P_2 , located around -120°C and 30°C , respectively, as shown in Figs. 23 and 25. Curves (1) and (3) in Fig. 23 show the TSC and the TL of the photoelectret obtained under a collecting bias, and curve (2) shows the TSC under the same conditions, except that in this case the specimen had received no prior illumination. The latter TSC may contain polarization and conduction currents, especially at higher temperatures. Thus, the difference between curves (1) and (2) should be ascribed to the effect of illumination. That is, photogenerated charge carriers are immobilized and trapped after drifting a certain distance at low temperatures (-196°C), and are then thermally released during the heating process and drift under the collecting bias. On the other hand, the TL also showed a peak and a shoulder around the same temperatures as those at which the TSC showed peaks. Since TL should originate from the recombination of thermally-detrapped electrons or holes and photogenerated positive or negative molecular ions, these facts support the conclusion that the TSC peaks P_1 and P_2 in the photoelectrets resulted from the thermal release of charge carriers from carrier traps. The following results, however, suggest that the detrapping processes depend on local motions of PEN

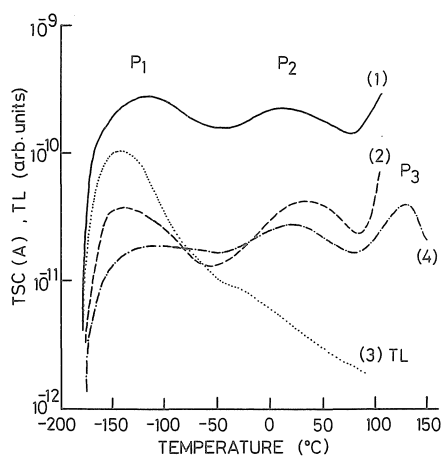


Fig. 23. TSC and TL obtained under various conditions as given in text. Curves (1), (2) and (3). $E_d = 2.5 \times 10^5$ V/cm, $E_c = 2.5 \times 10^5$ V/cm.

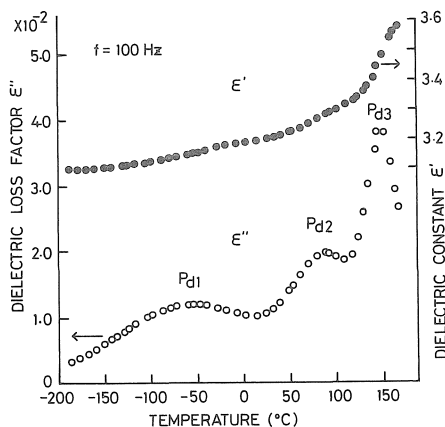


Fig. 24. Temperature dependence of dielectric constant ϵ' and loss factor ϵ'' at 100 Hz.

molecules. Curve (4) shows the TSC obtained from a thermoelectret polarized at 120°C by applying a field (6×10^4 V/cm) for 10 min; it has three peaks, P_1 , P_2 and P_3 . Both peak P_1 and peak P_2 were observed at almost the same temperatures as those at which they were obtained for the photoelectret.

In order to discuss these TSC peaks P_1 , P_2 and P_3 , the dielectric properties were measured. The temperature dependences of the dielectric constant ϵ' and the loss factor ϵ'' at 100 Hz are shown in Fig. 24. The loss factor ϵ'' showed three peaks, P_{d1} , P_{d2} and P_{d3} , at -60, 90, and 150°C respectively. Peak P_{d3} is thought to be related to the α relaxation because of its temperature and activation energy (130 kcal/mol), and to correspond to the TSC peak P_3 in thermoelectrets. The remaining peaks, P_{d2} and P_{d1} , are associated with the β and γ relaxations, which are thought to be related to the molecular motions of naphthalene groups, and methylene groups as in the

case of PET.⁹⁾ These peaks P_{d1} and P_{d2} are considered to correspond respectively, to the TSC peaks P_1 and P_2 obtained from the thermoelectrets, though there are substantial differences between the peak temperature of the TSC and that of the loss factor ϵ'' . This may be explained by the shift in the peak temperature of the loss factor at a low frequency comparable to that of the TSC measurement. To compare the peak temperatures of the TSC with that of the loss factor ϵ'' , the equivalent frequency of the TSC measurement was calculated from the equation²²⁾

$$f = E\beta/2\pi k T_m^2, \quad (6)$$

where E is the activation energy, β is the rate of temperature rise, k is Boltzmann's constant and T_m is the peak temperature of the TSC. The frequencies for peaks P_1 , P_2 and P_3 ranged from 10^{-3} ~ 10^{-4} Hz. Extrapolation of the peak temperatures of the loss factor to low frequencies of 10^{-3} ~ 10^{-4} Hz resulted in a good agreement between the peak temperatures of the TSC and the loss factor. Furthermore, the dependence of the TSC peaks P_1 , P_2 and P_3 on the forming field, was linear over a wide range of field (~ 1 MV/cm). These facts suggest that the TSC peaks P_1 , P_2 and P_3 in the thermoelectret resulted from the depolarization of the dipoles.

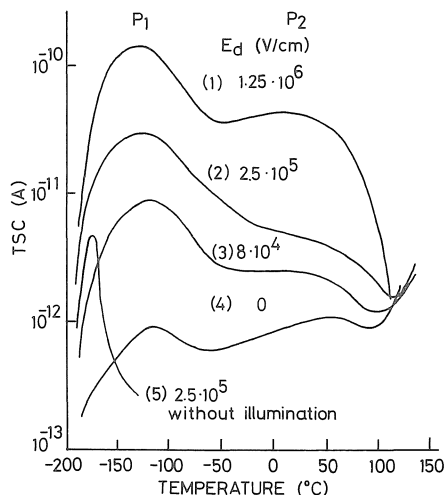


Fig. 25. Short-circuit TSC obtained from photoelectrets formed under various forming fields E_d .

Figure 25 shows the short circuit TSC's obtained from photoelectrets formed under various drift biases (curves 1~4), and from the electret formed by applying a field (0.25 MV/cm), but no illumination (curve 5). The last curve, curve (5), is thus considered to be composed of the depolarization current of dipoles oriented at 77 K. Thus, the effect of illumination is specified by the difference between curves (2) and (5). Consequently, the short-circuit TSC from the photoelectret can be considered to be due mainly to

released carriers, and it shows peaks in the same temperature region as that shown in Fig. 23.

The activation energies of the TSC's from the thermoelectret and photoelectret were estimated using the partial heating method described by Creswell and Perlman,²³⁾ and were found to be 0.1 eV and 0.5 eV, respectively, for the TSC peaks P_1 and P_2 from the photoelectret. These values coincided well with those obtained from the thermoelectret, as shown in Fig. 26. Similar results were obtained in polymers such as polyethylene terephthalate,²⁴⁾ poly-p-xylylene²⁵⁾ and polyethylene.²⁶⁾ Thus, these results suggest that the detrapping of charge carriers is strongly affected by molecular motions and that the trap depth of carrier traps in polymers determined by the thermal method is an apparent depth modified by the molecular motions.

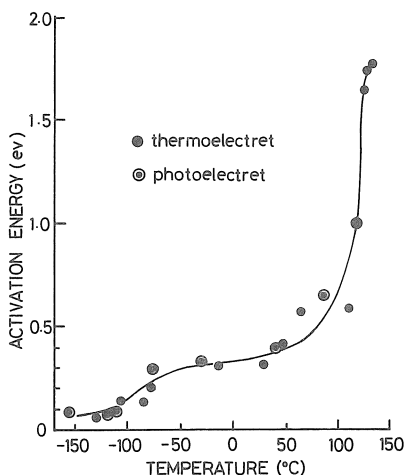


Fig. 26. Apparent activation energies obtained from thermoelectret (●) and photoelectret (⊙).

Some experiments were carried out to determine the carrier source and the type of dominant carriers. To clarify whether the carrier is injected from the electrodes or generated in the bulk of the specimen, the dependence of the TSC and TL on the type of electrode was investigated in photoelectrets with Au or Al electrodes.

Figure 27 shows the results obtained on photoelectrets formed by illumination with strongly-absorbed light of 360 nm. No appreciable differences were detected in the TSC and TL of photoelectrets with Au or Al electrodes. Furthermore, no significant effects of the polarity of the forming field were observed in the TSC and TL from the photoelectret, though the light was strongly absorbed at the surface layer. These results suggest that the carriers are supplied through optical excitation in the bulk, but not by injection from the electrodes, and that the electrons and holes contribute to the TSC to the same degree.

Further experiments on photoconduction are now

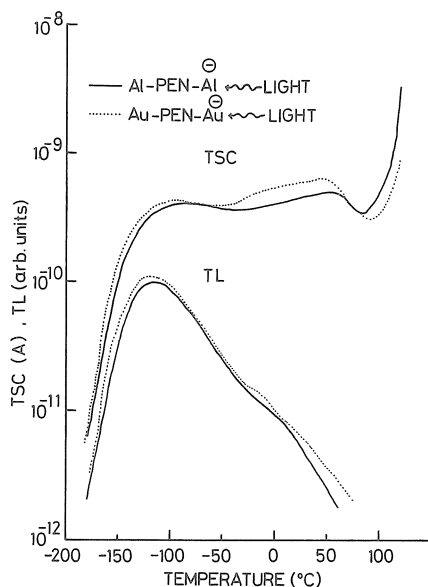


Fig. 27. Dependence of TSC and TL on electrodes obtained from photoelectret. $E_d = 3 \times 10^5$ V/cm, $E_c = 3 \times 10^5$ V/cm.

in progress to decide whether electrons or holes are the main contributors to the conduction.

4 Summary

Carrier traps in polymers were investigated by analysing their TSC and TL to clarify the electronic properties of insulating polymeric materials. Three different excitation sources were utilized for forming the electrets. Their characteristics were summarized in the following, (1) field injection: carrier injection occurs easily from the Al cathode into polymers at low fields (3×10^5 V/cm). The TSC's, however, are complicated, because polarization of dipoles and ions are induced by the electric field, simultaneously. (2) Electron beam irradiation: electron can be injected into all of polymers irrespectively of their molecular structures. The penetration depth of incident electron is easily controlled by the accelerating voltage. (3) photo-carrier generation: this method can be generally applied to all of photoconducting materials. There have been not so much reports on the photoelectret of insulating polymers. Carriers are excited homogeneously in wide area by illumination of strongly absorbed light producing the TSC with good reproducibility. More useful points of the method are that the special group in molecular chains can be excited selectively by the incident light with their excitation wavelength.

References

- 1) T. Hino: J. Inst. Elect. Engrs. Japan. **93-A** (1973) 465 [in Japanese].

- 2) J. Vanderschueren : J. Polym. Sci. Polym. Phys. Ed. **15** (1977) 873.
- 3) Y. Takai, T. Osawa, T. Mizutani, M. Ieda and K. Kojima : Japan. J. appl. Phys. **15** (1976) 1597.
- 4) S. Nakamura, G. Sawa and M. Ieda : Japan. J. appl. Phys. **16** (1977) 2165.
- 5) T. Mizutani, Y. Suzuoki and M. Ieda : J. Inst. Engrs. Japan **96-A** (1976) 419 [in Japanese].
- 6) B. Gross, G. M. Sessler and J. E. West : J. Appl. Phys., **45**, 2841 (1974)
- 7) F. Kaneko and T. Hino : J. Inst. Elect. Engrs. Japan **98-A** (1978) 45 [in Japanese].
- 8) T. Hino and Y. Kitamura : J. Inst. Elect. Engrs. Japan **95-A** (1975) 71 [in Japanese].
- 9) K. H. Illers and H. Breuer : J. Colloid Sci. **18** (1963) 1.
- 10) A. C. Lilly, Jr. Rosemary, M. Henderson and P. S. Sharp : J. appl. Phys. **41** (1970) 2001.
- 11) T. Nishitani, K. Yoshino and Y. Inuishi : J. Inst. Elect. Engrs. Japan **96-A** (1976) 381 [in Japanese].
- 12) K. Amakawa and Y. Inuishi : J. Inst. Elect. Engrs. Japan **93-A** (1973) 533 [in Japanese].
- 13) I. Chen : J. Appl. Phys., **47**, (1976) 2988.
- 14) M. Zielinski and M. Somoć : J. Phys. D : Appl. Phys., **10**, (1977) L105.
- 15) D. Phillips and J. C. Schug : J Chem. Phys., **50**, (1969) 3297.
- 16) P. R. Cheung and C. W. Roberts : Appl. Polym. Sci., **24**, (1979) 1809.
- 17) N. S. Allen and J. F. Mckellar : Makromol. Chem., **179**, (1978) 523.
- 18) G. F. J. Garlick and A. F. Gibson : Proc. Roy. Soc. London, **60**, (1948) 574.
- 19) M. J. Berger and S. M. Seltzer : NASA SP, (1964) 3012.
- 20) Y. Takai, K. Mori, T. Mizutani and M. Ieda : J. Phys. D., **11**, (1978) 991.
- 21) Y. Takai, T. Osawa, K. C. Kao, T. Mizutani and M. Ieda ; Japan. J. appl. Phys. **14** (1975) 473.
- 22) J. Van. Turnhout : *Electrets*, ed. G. M. Sessler (Springer-Verlag, Berlin-Heidelberg-New York, 1980) p. 132.
- 23) R. A. Creswell and M. M. Perlman : J. Appl. Phys. **41** (1970) 2365.
- 24) Y. Takai, T. Osawa, T. Mizutani and M. Ieda : Jpn. J. Appl. Phys. **16** (1977) 1933.
- 25) T. Mizutani, K. Ishii, Y. Takai and M. Ieda : Jpn. J. Appl. Phys. **19** (1980) 1073.
- 26) A. Charlesby and R. H. Partridge : Proc. R. Soc. London A **271** (1973) 170.

(Received January 17th 1984)